



Contents lists available at ScienceDirect

## Bioorganic &amp; Medicinal Chemistry

journal homepage: [www.elsevier.com/locate/bmc](http://www.elsevier.com/locate/bmc)

## Galantamine derivatives with indole moiety: Docking, design, synthesis and acetylcholinesterase inhibitory activity

Mariyana Atanasova<sup>a,†</sup>, Georgi Stavrakov<sup>a,†</sup>, Irena Philipova<sup>b,†</sup>, Dimitrina Zheleva<sup>a</sup>, Nikola Yordanov<sup>a</sup>, Irini Doytchinova<sup>a,\*</sup>

<sup>a</sup> Faculty of Pharmacy, Medical University of Sofia, 2 Dunav Str., 1000 Sofia, Bulgaria

<sup>b</sup> Institute of Organic Chemistry with Centre of Phytochemistry, Bulgarian Academy of Sciences, Acad. G. Bonchev Str. 9, 1113 Sofia, Bulgaria

## ARTICLE INFO

## Article history:

Received 11 June 2015

Revised 20 July 2015

Accepted 25 July 2015

Available online xxx

## Keywords:

Acetylcholinesterase inhibitors

Galantamine

Molecular docking

GoldScore

Indole

Amyloid beta peptide

## ABSTRACT

The inhibitors of acetylcholinesterase are the main therapy against Alzheimer's disease. Among them, galantamine is the best tolerated and the most prescribed drug. In the present study, 41 galantamine derivatives with known acetylcholinesterase inhibitory activities expressed as IC<sub>50</sub> were selected from the literature and docked into a recombinant human acetylcholinesterase by GOLD. A linear relationship between GoldScores and pIC<sub>50</sub> values was found and used to design and predict novel galantamine derivatives with indole moiety in the side chain. The four best predicted compounds were synthesized and tested for inhibitory activity. All of them were between 11 and 95 times more active than galantamine. The novel galantamine derivatives with indole moiety have dual site binding to the enzyme—the galantamine moiety binds to the catalytic anionic site and the indole moiety binds to peripheral anionic site. Additionally, the indole moiety of one of the novel inhibitors binds in a region, close to the peripheral anionic site of the enzyme, where the Ω-loop of amyloid beta peptide adheres to acetylcholinesterase. This compound emerges as a promising lead compound for multi-target anti-Alzheimer therapy not only because of the strong inhibitory activity, but also because it is able to block the amyloid beta deposition on acetylcholinesterase.

© 2015 Elsevier Ltd. All rights reserved.

### 1. Introduction

Alzheimer's disease (AD) is the most common type of dementia worldwide.<sup>1</sup> The hallmark pathologies of AD are the progressive accumulation of the protein fragment beta-amyloid (plaques) outside neurons in the brain and twisted strands of the protein tau (tangles) inside neurons. These changes are eventually accompanied by the damage and death of neurons. Early symptoms of AD are difficulty remembering recent conversations, names or events, apathy and depression. Later symptoms include impaired communication, disorientation, confusion, poor judgment, behavior changes, and difficulty speaking, swallowing and walking. AD is ultimately fatal.

The current treatment of AD reduces dementia symptoms but does not arrest or reverse the underlying neurodegenerative disorder. There are only two classes of drugs approved for AD treatment: acetylcholinesterase inhibitors (AChEIs) and inhibitors of N-methyl-D-aspartate (NMDA) receptors. The available AChEIs are

donepezil, rivastigmine and galantamine, while the NMDA inhibitors are represented by one drug—memantine. Although there are many successful therapeutic strategies tested in animal models, most of them have failed in humans.<sup>2</sup> Recently, the current status of anti-AD therapies has been extensively reviewed.<sup>2–6</sup>

The neurotransmitter acetylcholine (ACh) plays a key role in memory and cognition. According to the 'cholinergic hypothesis',<sup>7</sup> the death of neurons strongly diminishes the levels of ACh in cholinergic brain synapses. The inhibition of the enzyme acetylcholinesterase (AChE) which hydrolyses ACh directly enhances the levels of ACh and improves the cholinergic transmission. Additionally, it was found that AChE accelerates the aggregation of amyloid-β peptide (Aβ) which is the main constituent of senile plaques and a major neurotoxic agent.<sup>8–10</sup> AChE forms stable neurotoxic complexes with Aβ. The complexes induce Aβ-dependent deregulation of intracellular Ca<sup>2+</sup> in hippocampal neurons, mitochondrial dysfunction, neurite network dystrophy and apoptosis.<sup>10</sup>

The binding site of recombinant human AChE (*rhAChE*) consists of several domains.<sup>11–15</sup> The catalytic site lies on the bottom of 20 Å deep and narrow binding gorge. It consists of the catalytic triad: Ser203, Glu334 and His447. The anionic domain binds the

\* Corresponding author.

E-mail address: [idoitchinova@pharmfac.net](mailto:idoitchinova@pharmfac.net) (I. Doytchinova).

† Authors with equal contributions.

quaternary trimethylammonium choline moiety of ACh. Despite its name, it does not contain any anionic residues but only aromatic ones: Trp86, Tyr130, Tyr337 and Phe338. They are involved in cation– $\pi$  interactions with the protonated head of ACh. The acyl pocket consists of two bulky residues: Phe295 and Phe297, and it determines the selective binding of ACh by preventing the access of larger choline esters. The oxyanion hole hosts one molecule of structural water and consists of Gly121, Gly122 and Ala204. The water molecule bridges the binding between enzyme and substrate by hydrogen-bond networking and stabilizes the substrate tetrahedral transition state. Finally, the peripheral anionic site (PAS) lies at the entrance to binding gorge. It is composed of five residues: Tyr72, Asp74, Tyr124, Trp286 and Tyr341. PAS allosterically modulates catalysis<sup>16</sup> and is implicated in non-cholinergic functions as amyloid deposition,<sup>17</sup> cell adhesion and neurite outgrowth.<sup>18,19</sup> It was found that the A $\beta$  peptide binds close to PAS and the blockade of PAS prevents the AChE-induced A $\beta$  aggregation.<sup>17</sup> This pivotal finding prompted the design of novel AChEIs with dual binding moieties—one blocking the catalytic site at the bottom of the gorge and one blocking the PAS.<sup>20–25</sup>

The BLAST alignment of AChEs from human, rat, rabbit and *Torpedo californica* showed that the main residues forming the binding site are conserved (data not shown). The only difference concerns Tyr337 which in *T. californica* mutates to Phe (Phe330).<sup>26</sup> The X-ray data show that the binding of galantamine in rhAChE is similar to that observed in tAChE with one additional hydrogen bond formed between the tertiary amine and Tyr337.<sup>27</sup> Donepezil, however, binds differently to rhAChE than it does to tAChE.<sup>27</sup>

Galantamine (GAL) is an alkaloid initially isolated from the bulbs and flowers of *Galanthus caucasicus*, *Galanthus woronowii* (Amaryllidaceae) and related genera.<sup>28</sup> Paskov first developed GAL as an industrial drug under the trade name Nivalin (Sopharma, Bulgaria).<sup>29</sup> It has been used for treatment of myasthenia gravis, myopathy, residual poliomyelitis paralysis syndromes, sensory and motor disorders of CNS, and decurarization.<sup>30–34</sup> Because of its ability to cross the blood–brain barrier and to affect the central cholinergic function, in 1980s GAL was investigated for treatment of Alzheimer's disease (AD) and in 2000 was approved for use in Europe, United States and Asia.<sup>35–37</sup>

In addition to its AChE inhibiting ability, GAL has been identified as an allosteric modulator of nicotinic acetylcholine receptors (nAChRs).<sup>38–41</sup> The stimulation of nAChRs can increase intracellular Ca<sup>2+</sup> levels and facilitate noradrenaline release; both effects enhance the cognitive brain function.<sup>42</sup> Recently, Takata et al. have demonstrated that treatment of rat microglia with GAL significantly enhanced microglial amyloid- $\beta$  (A $\beta$ ) phagocytosis and facilitated A $\beta$  clearance in brains of rodent AD models.<sup>43</sup> This multiple-target action of GAL makes it a most valuable drug for AD treatment and prompts the synthesis of novel GAL derivatives with improved binding to AChE.<sup>44–50</sup> Several series of GAL derivatives with dual site binding to the enzyme have been prepared and tested.<sup>46,51–53,24</sup> All of them showed good AChE inhibitory activities.

In the present study, we applied molecular docking on two series of GAL derivatives binding to AChE and we derived a quantitative relationship between the docking-based scores and AChE inhibitory activities. This relationship was used to predict the activities of newly designed galantamine derivatives with indole moiety ending the side chain attached to N-atom. The indole moiety was selected as suitable for binding to the aromatic residues in PAS because of its ability to take part in hydrophobic and  $\pi$ – $\pi$  interactions.<sup>54,55</sup> The best four predicted compounds were synthesized and tested. All of them showed activity higher than that of GAL. The most active derivative was 95 times more active than GAL. The prolongation of the side chain at N-atom increases the

interactions between the ligand and AChE and makes possible the inhibition of A $\beta$  peptide binding to PAS.

## 2. Results and discussion

### 2.1. Molecular docking of galantamine derivatives on rhAChE

Two series (A and B) of 41 GAL derivatives in total with AChE inhibitory activities expressed as IC<sub>50</sub> values were selected from the literature<sup>56,57</sup> and used to derive a relationship between docking scores and activities. The structures and IC<sub>50</sub> values of the studied compounds are given in [Supplementary data](#). The compounds were docked into the rhAChE (pdb code: 4EY6)<sup>27</sup> by GOLD v. 5.1.<sup>58</sup> The molecular docking protocol was optimized in several steps as described in Methods. At each step of the docking protocol optimization, the correlation between the docking scores and the pIC<sub>50</sub> (–logIC<sub>50</sub>) values of the compounds was evaluated by the Pearson's correlation coefficient *r*. The highest correlation coefficient *r* = 0.826 was achieved at the following settings: GoldScore fitness function, flexible binding site with radius of 10 Å and a water molecule inside. The relationship between GoldScores and pIC<sub>50</sub> is given below and illustrated in [Figure 1](#).

$$\text{pIC}_{50} = 0.083\text{GoldScore} - 1.723.$$

### 2.2. Design of novel galantamine derivatives and AChE inhibitory activity prediction

Ten novel galantamine derivatives with indole moiety ending the side chain attached to N-atom were designed and docked on the rhAChE using the optimized docking protocol derived previously. The indole moiety was selected as suitable for binding to the aromatic residues in PAS. The average GoldScores of three runs were used to predict the pIC<sub>50</sub> values according to the above relationship. The top four best predicted compounds were synthesized and tested for AChE inhibitory activity. The structures of the newly designed compounds are given in [Figure 2](#), while their GoldScores and predicted pIC<sub>50</sub> values—in [Table 1](#).

### 2.3. Synthesis of the best predicted galantamine derivatives

Our synthetic strategy towards the target molecules focused on the preparation of bromine-containing building blocks and their subsequent substitution with *N*-demethylated galantamine.

Construction of the required indole based building blocks was performed by applying simple and effective synthetic procedures ([Scheme 1](#)). Compound **3a** was prepared by reaction of reductive alkylation of 1*H*-indol-5-amine with readily available 4-(6-bromohexyloxy)benzaldehyde<sup>22</sup> in the presence of NaBH(OAc)<sub>3</sub>. The desired product was obtained in quantitative yield after flash column chromatography. Treatment of 1*H*-indol-5-ol with commercially available 1,6-dibromohexane in the presence of potassium carbonate in CH<sub>3</sub>CN at 60 °C for 24 h gave rise to compound **3b** in 68% yield after purification by flash chromatography. The formation of the products **3c** and **3d** was accomplished by procedures developed for peptide synthesis. The reaction of 1*H*-indol-5-amine with commercially available 6-bromohexanoic acid in the presence of 1-ethyl-3-(3-dimethylaminopropyl)carbodiimide (EDC) and 1-Hydroxybenzotriazole hydrate (HOBT) as coupling reagents afforded **3c**. Following the same protocol for *L*-tryptophan methyl ester hydrochloride and in the presence of *N,N*-diisopropylethylamine (DIPEA) we synthesized amide **3d**. The products were obtained in excellent yields and purity after flash column chromatography.

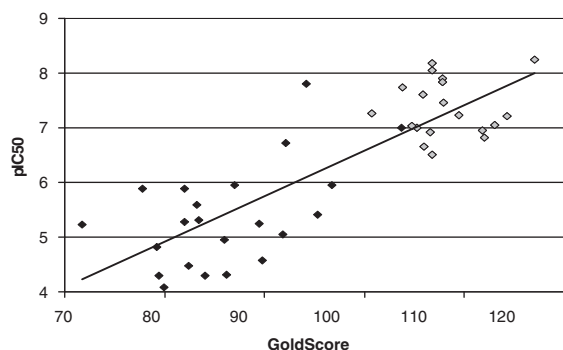


**Figure 1.** Relationship between GoldScores and  $pIC_{50}$  of 41 galantamine derivatives,  $r = 0.826$ . The compounds from series A and B are given with black and grey diamonds, respectively.

An efficient *N*-selective demethylation of galantamine to norgalantamine **2** was accomplished by a non-classical *Polonovski* reaction using iron(II) sulfate heptahydrate (Scheme 2).<sup>59</sup> Alkylation of norgalantamine **2** with the indole-based bromides **3a–d** was realized via nucleophilic substitutions.<sup>57</sup> Thus, heating of **2** with bromides **3a–d** in acetonitrile in the presence of  $K_2CO_3$  as a base for 24 h afforded the targeted compounds **1a–d** in good yields and excellent purity after flash column chromatography (Scheme 2). The structures of the newly synthesized compounds were proven by NMR spectroscopy and elemental analysis.

#### 2.4. Assessment of AChE inhibitory activity

The inhibitory potential of the novel GAL derivatives against *T. californica* AChE (*tAChE*) was tested according to the methodology developed by Ellman et al.<sup>62</sup> with some modifications.<sup>61</sup> GAL was used as a positive control and the enzyme activity was calculated at  $IC_{50} = 1.07 \mu M$  for GAL. The  $IC_{50}$  values ( $\mu M$ ) of the novel compounds are shown in Table 1. Compounds **1a–c** demonstrated the highest acetylcholinesterase inhibitory activity, with similar  $IC_{50}$  values ( $0.011 \mu M$ ,  $0.012 \mu M$  and  $0.015 \mu M$ , respectively), while compound **1d** was less active ( $0.094 \mu M$ ). All newly synthesized derivatives showed AChE inhibitory activities between 11 and 95 times higher than this of GAL ( $IC_{50} = 1.070 \mu M$ ). The differences between predicted and experimental  $pIC_{50}$  values of the novel compounds were less than one log unit.

#### 2.5. Interactions between the new compounds and rhAChE

The interactions between the novel GAL derivatives and *rhAChE* were analyzed by YASARA.<sup>62</sup> Four types of interactions were

considered: hydrogen bonds, hydrophobic,  $\pi$ – $\pi$  and cation– $\pi$  interactions. They are visualized on the highest-scored pose of the complex compound **1a**–*rhAChE*. The compound **1a** is the ligand with the highest AChE affinity among the newly synthesized ligands ( $IC_{50} = 0.011 \mu M$ ).

The single water molecule in binding site is situated deep in the bottom of the gorge and is involved in a hydrogen-bond network connecting ligand and enzyme (Fig. 3a). It acts as hydrogen-bond acceptor with Gly122 and Ala204 from the oxyanion hole and as a hydrogen-bond donor with the ligand hydroxyl and methoxy group. The ligand itself is involved in additional three hydrogen bonds. The protonated nitrogen is a donor in the hydrogen bond with Tyr337 from the anionic site; the hydroxyl group acts as a donor in the bonding with Glu202; the oxygen atom from the methoxy group is an acceptor in the bonding with Ser203 from the catalytic domain. No hydrogen bonds exist along the *N*-side chain.

The hydrophobic interactions inside the binding gorge are visualized in Figure 3b. The GAL moiety makes hydrophobic interactions with Trp86 and Phe295. The side chain interacts with Tyr72. The aromatic ring from the GAL moiety is involved in  $\pi$ – $\pi$  interactions with Tyr124 and Phe297 (Fig. 3c). Trp286 is in a good position of stacking with the phenyl ring from GAL side chain and to make a  $\pi$ – $\pi$  interaction (Fig. 3c). Finally, the protonated *N*-atom of GAL moiety interacts with Trp86 (Fig. 3d).

View of the complex **1a**–AChE in profile of the binding gorge is given in Figure 4 (**1a** is given in blue). The binding gorge is totally filled by the ligand and even part of the indole moiety protrudes outside the gorge. Recent studies reveal that *N*-substituents with long chains are favourable for AChE inhibitory activity because of the ability to interact with the PAS.<sup>46,51–53,24,54–57</sup>

In order to explore the importance of PAS for amyloid beta ( $A\beta$ ) deposition on AChE, a complex was generated between AChE and  $A\beta$  peptide by RosettaDock<sup>63</sup> as described in Materials and methods. The complex with the lowest score was selected as the most probable. In this complex, the  $\Omega$ -loop of  $A\beta$  is bound in a region, close to the PAS of AChE (Fig. 4). This pose coincides with the AChE– $A\beta$  binding mode, identified by Inestrosa in 2001.<sup>17</sup> The superposed complexes **1a**–AChE, **1c**–AChE and AChE– $A\beta$  are given in Figure 4. It is evident that the phenyl ring of **1a** and the indole ring of **1c** bind inside the PAS, while the indole moiety of **1a** and the  $\Omega$ -loop of  $A\beta$  bind in a region, proximal to PAS.

In Figure 5 are given superposed main residues of PAS (Tyr72, Asp74, Tyr124, Trp286 and Tyr341) from the complexes AChE– $A\beta$  (in yellow) and **1a**–AChE (in cyan). Four of the five residues, that is, Tyr72, Asp74, Tyr124 and Tyr341, adopt almost the same conformations in both complexes. Only residue Trp286 makes a significant shift. In the complex AChE– $A\beta$ , Trp286 takes an ‘open’

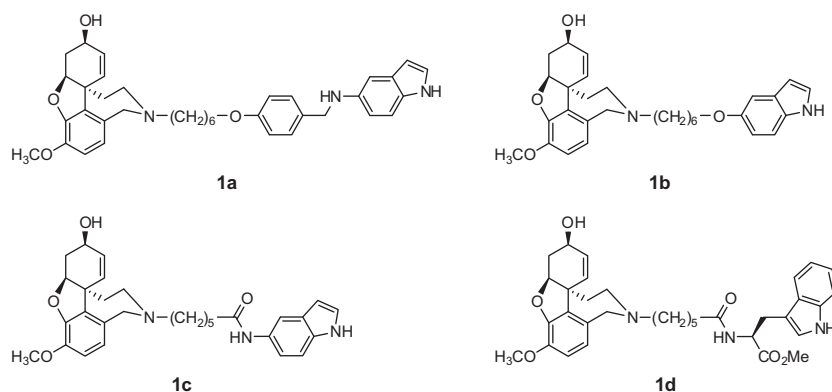
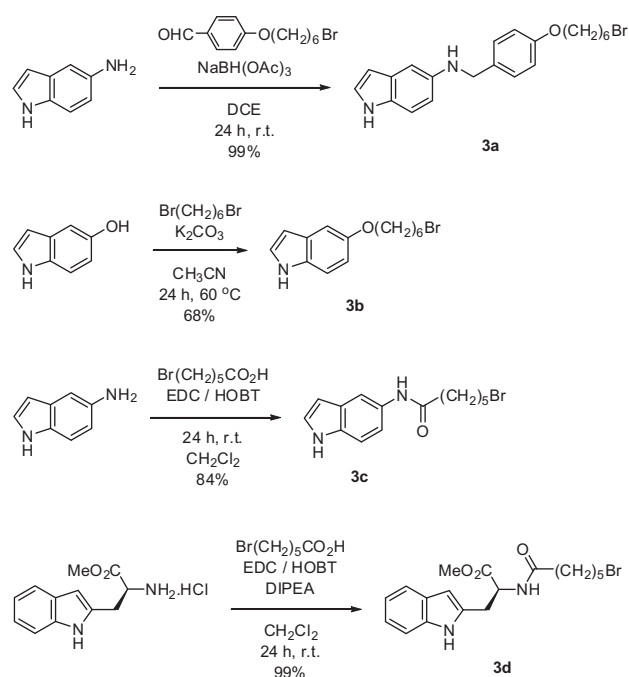


**Figure 2.** Structures of the newly designed GAL derivatives.

**Table 1**  
GoldScores, predicted and experimental pIC<sub>50</sub> values of the newly designed and synthesized GAL derivatives

Compd	GoldScore	pIC <sub>50</sub> (pred)	IC <sub>50</sub> μM (exp) tAChE	Times more active than GAL	pIC <sub>50</sub> (exp)	pIC <sub>50</sub> (pred)–pIC <sub>50</sub> (exp)
<b>1a</b>	119.15	8.166	0.011 ± 0.0004	95	7.949	0.218
<b>1b</b>	112.32	7.599	0.012 ± 0.0021	93	7.938	–0.339
<b>1c</b>	109.06	7.329	0.015 ± 0.0003	72	7.829	–0.501
<b>1d</b>	113.89	7.730	0.094 ± 0.0118	11	7.027	0.703
GAL HBr	73.59	4.385	1.070 ± 0.1559	1	5.971	–1.586

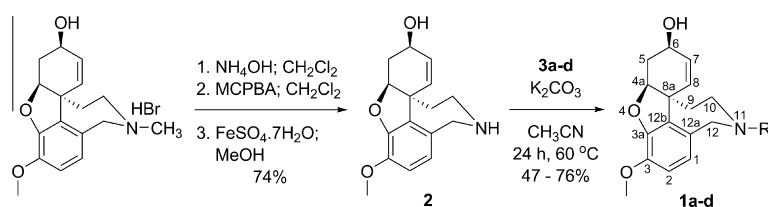
\* Recalculated at GAL IC<sub>50</sub> = 1.07 μM.



**Scheme 1.** Synthesis of indole based building blocks.

position and makes  $\pi$ – $\pi$  interaction with Phe4 from A $\beta$  (given as AbPhe4). In the complex **1a**–AChE, Trp286 moves toward the phenyl ring of **1a** because of the  $\pi$ – $\pi$  stacking and reduces the cavity of PAS ('closed' position). The 'closed' position of Trp286 prevents from interaction with A $\beta$  Phe4. Additionally, the indole moiety of **1a** fills the region, proximal to PAS, where the  $\Omega$ -loop of A $\beta$  adheres to AChE.

Although the novel galantamine derivatives have close AChE inhibitory activities, compound **1a** emerges as the most promising lead compound for multi-target anti-Alzheimer therapy not only because of the strong AChE inhibitory activity, but also because it is able to block the A $\beta$  deposition on AChE. The experimental confirmation of this hypothesis is in progress.



**Scheme 2.** Synthesis of the target molecules via norgalantamine.

### 3. Conclusion

The molecular docking study on GAL derivatives binding to AChE shows that the GoldScores of the inhibitor–AChE complexes derived by an optimized docking protocol correlate well with the inhibitory activities of the studied compounds. This docking protocol is able to predict the activities of newly designed AChE inhibitors with indole moiety ending the side chain attached to N-atom. The synthesized and tested novel compounds confirm the predictions. The docked complexes reveal that the novel inhibitors show dual site binding to the enzyme—the galantamine moiety binds to the catalytic anionic site and the indole moiety binds to peripheral anionic site. The indole moiety of one of the inhibitors binds in the same region, where A $\beta$  adheres to AChE.

### 4. Materials and methods

#### 4.1. Datasets and molecular docking protocol

Two series of 41 GAL derivatives with AChE inhibitory activities expressed as IC<sub>50</sub> values were selected from the literature<sup>56,57</sup> and used as a training set to derive a relationship between docking scores and IC<sub>50</sub>s. The structures are given in [Supplementary material](#). All IC<sub>50</sub> values are used in *p*-units (–log).

Recently published X-ray structure of rhAChE in complex with galantamine (GAL) (pdb id: 4EY6, R = 2.15 Å)<sup>27</sup> was used as a template for docking calculations by GOLD v. 5.1.<sup>58</sup> GOLD is a docking tool based on a genetic algorithm and it has proven successful in virtual screening, lead optimisation, and identification of the correct binding mode of active molecules.<sup>64,65</sup> GOLD takes into account the flexibility of the ligand as well as the flexibility of the residues in the binding site.

The molecular docking protocol was optimized in several steps. Initially, the protocol consisted of rigid protein, flexible ligand, radius of the binding site 6 Å and one water molecule (HOH846) kept within the binding site. According to the X-ray structure of the complex GAL–rhAChE,<sup>27</sup> only one water molecule was left in the binding gorge, making a hydrogen bond network between GAL, Ser203, Gly121 and Gly122. This initial protocol was used to select a scoring function (SF) among the four available SFs in GOLD: ChemPLP, ChemScore, GoldScore and ASP. Next, the influence of structural water and flexible protein binding site were examined. Ten amino acids from the binding site situated in a close proximity to the binding ligands were selected as flexible. These were Tyr72, Asp74, Trp86, Tyr124, Ser125, Trp286, Phe297, Tyr337, Phe338 and Tyr341. Finally, the optimal radius of the binding site was adjusted. Each run generated 10 docking poses. The poses were ranked by two criteria: (1) highest fitness score and (2) rmsd (root mean square deviation) lower than 1.5 Å. These poses that did not meet these criteria were assigned as 'Non-docked'. Each docking run was repeated three times and the average fitness score was used for correlation with the pIC<sub>50</sub>.

At each step of the docking protocol optimization, the correlation between the docking scores and the pIC<sub>50</sub> (–log IC<sub>50</sub>) values of the training compounds was evaluated by the *Pearson's*

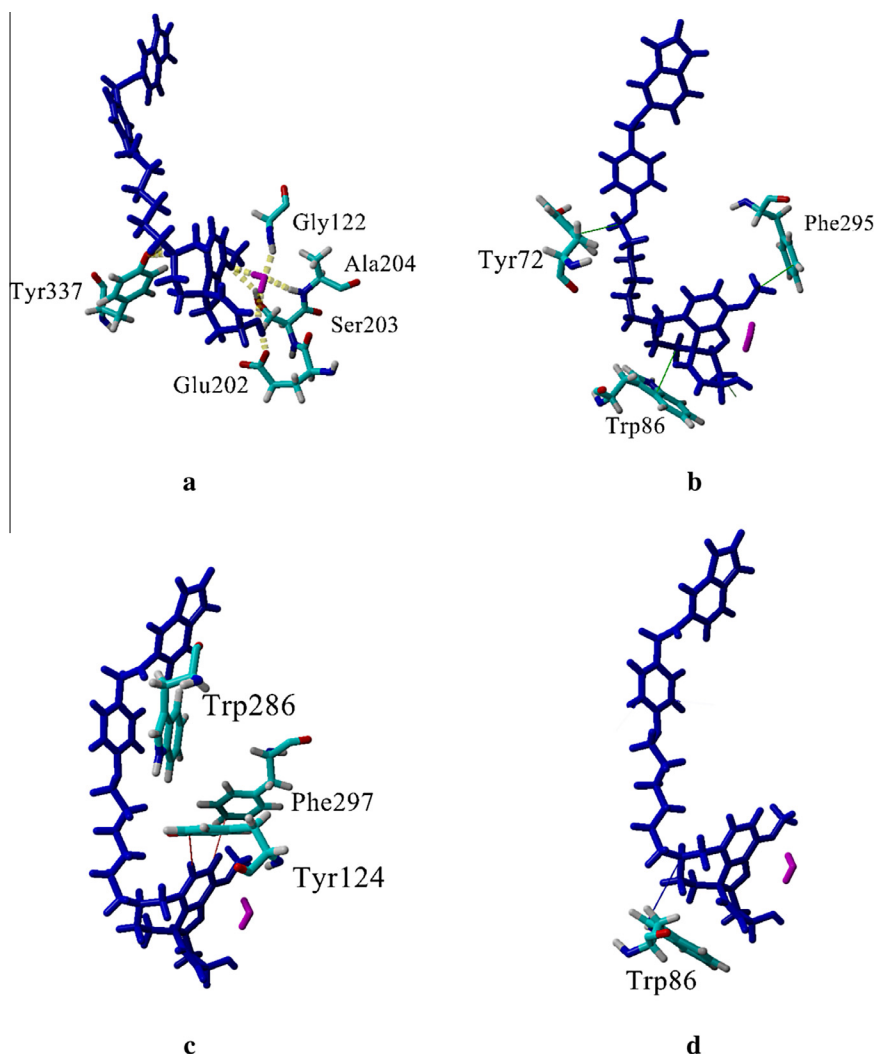


**Figure 3.** (a) Hydrogen bonds (yellow dotted lines) between ligand (blue sticks), water molecule (purple sticks) and AChE residues (sticks colored by element). (b) Hydrophobic interactions (green lines). (c)  $\pi$ - $\pi$  interactions (red lines). (d) Cation- $\pi$  interaction (blue lines).

correlation coefficient  $r$ . Some compounds were not docked at the tested conditions. Apart from  $r$ , the number of docked structures was considered during the optimization.

RosettaDock server<sup>63</sup> was used to generate the complex AChE- $\text{A}\beta$  peptide. The docking partners were uploaded as two separate pdb files: 4EY6<sup>27</sup> for AChE and 1AML<sup>66</sup> for  $\text{A}\beta$ . The complex with the lowest score was selected as the most probable.

## 4.2. Synthesis

### 4.2.1. General

Reagents were commercial grade and used without further purification. Thin layer chromatography (TLC) was performed on aluminum sheets pre-coated with Merck Kieselgel 60 F<sub>254</sub> 0.25 mm (Merck). Flash column chromatography was carried out using Silica Gel 60 230–400 mesh (Fluka). Commercially available solvents for reactions, TLC and column chromatography were used after distillation (and were dried when needed). Melting points were determined in a capillary tube on SRS MPA100 OptiMelt (Sunnyvale, CA, USA) automated melting point system (uncorrected). Optical rotation ( $[\alpha]_D^{20}$ ) were measured on Perkin-Elmer 241 polarimeter. The NMR spectra were recorded on a Bruker Avance II+ 600 (600.13 for <sup>1</sup>H MHz and 150.92 MHz for <sup>13</sup>C NMR) and Bruker Avance DRX-250 (250.13 for <sup>1</sup>H MHz and 62.92 MHz

for <sup>13</sup>C NMR) spectrometer with TMS as internal standards for chemical shifts ( $\delta$ , ppm). <sup>1</sup>H and <sup>13</sup>C NMR data are reported as follows: chemical shift, multiplicity (s = singlet, d = doublet, t = triplet, q = quartet, br = broad, m = multiplet), coupling constants (Hz), integration, identification. The assignment of the <sup>1</sup>H and <sup>13</sup>C NMR spectra was made on the basis of DEPT, COSY and HSQC experiments. The spectra are given in [Supplementary material](#). Elemental analyses were performed by Microanalytical Service Laboratory of Faculty of Pharmacy, Medical University of Sofia, using Vario EL3 CHNS(O).

### 4.2.2. Synthesis of indole based building blocks

**4.2.2.1. N-(4-(6-Bromoheptyloxy)benzyl)-1H-indol-5-amine 3a.** A mixture of 1H-indol-5-amine (0.100 g, 0.757 mmol) and 4-(6-bromoheptyloxy)benzaldehyde (0.216 g, 0.757 mmol) in 8 ml 1,2-dichloroethane was stirred at rt for 30 min. Then NaBH(OAc)<sub>3</sub> (0.240 g, 1.136 mmol) was added and the reaction mixture was stirred at rt for 24 h. The reaction was quenched with sat. aq NaHCO<sub>3</sub>, the product was extracted with CH<sub>2</sub>Cl<sub>2</sub>, dried over Na<sub>2</sub>SO<sub>4</sub> and the solvent was evaporated under reduced pressure. Purification by flash-column chromatography on silica gel (hexane/EtOAc/Et<sub>3</sub>N = 2:1:0.5) gave 0.303 g (99%) of the product as white crystals, mp 86–89 °C. <sup>1</sup>H NMR (CDCl<sub>3</sub>, 600 MHz)  $\delta$  = 7.96 (br s, 2H, NH), 7.33–7.31 (m, 2H, arom.), 7.21–7.19 (m,

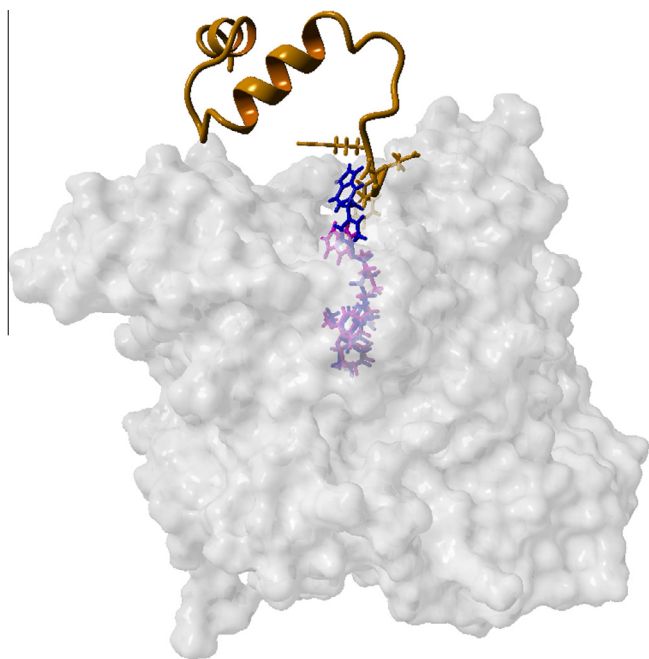


**Figure 4.** AChE binding gorge viewed in profile. AChE molecular surface is given in grey. Compounds **1a** (in blue) and **1c** (in magenta) are docked inside the gorge. The  $\beta$  peptide bound in the PAS is given in dark orange.

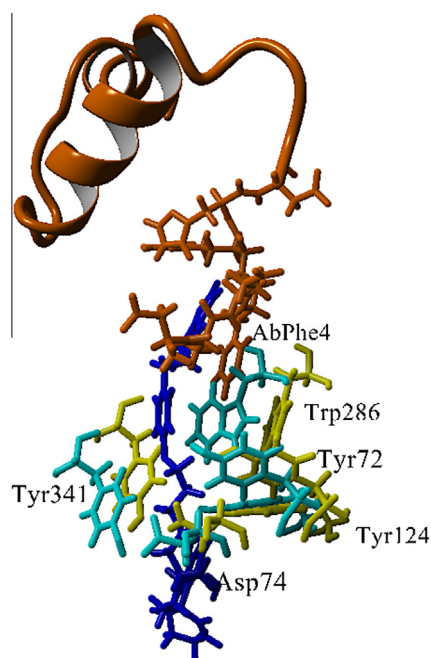


**Figure 5.** Superposed residues of PAS. The complex AChE- $\beta$  is given in yellow (AChE) and dark orange ( $\beta$ ). The complex **1a**-AChE is given in cyan (AChE) and blue (**1a**).

1H, arom.), 7.11–7.10 (m, 1H, arom.), 6.88–6.86 (m, 3H, arom.), 6.65 (dd,  $J_{h,h} = 8.6, 2.2$  Hz, 1H, arom.), 6.38–6.37 (m, 1H, arom.), 4.28 (s, 2H, HNCH<sub>2</sub>), 3.95 (t,  $J_{h,h} = 6.4$  Hz, 2H, OCH<sub>2</sub>), 3.42 (t,  $J_{h,h} = 6.8$  Hz, 2H, CH<sub>2</sub>Br), 1.90–1.88 (m, 2H, CH<sub>2</sub>), 1.80–1.78 (m, 2H, CH<sub>2</sub>), 1.51–1.50 (m, 4H, 2 CH<sub>2</sub>) ppm. <sup>13</sup>C NMR (CDCl<sub>3</sub>, 150.9 MHz)  $\delta = 158.17$  (1 arom. C), 142.28 (1 arom. C), 131.81 (1 arom. C), 130.09 (1 arom. C), 128.95 (2 arom. CH), 128.71 (1 arom. C), 124.39 (1 arom. CH), 114.47 (2 arom. CH), 112.17 (1 arom. CH), 11.58 (1 arom. CH), 102.35 (1 arom. CH), 101.79 (1 arom. CH),

67.69 (OCH<sub>2</sub>), 49.21 (HNCH<sub>2</sub>), 33.85 (CH<sub>2</sub>Br), 32.65 (CH<sub>2</sub>), 29.07 (CH<sub>2</sub>), 27.90 (CH<sub>2</sub>), 25.28 (CH<sub>2</sub>) ppm. C<sub>21</sub>H<sub>25</sub>BrN<sub>2</sub>O (401.34): calcd. C 62.85, H 6.28, N 6.98, found C 63.18, H 6.47, N 6.83.

**4.2.2.2. 5-(6-Bromohexyloxy)-1H-indole 3b.** To a solution of 1H-indol-5-ol (0.100 g, 0.750 mmol) in 15 ml CH<sub>3</sub>CN was added K<sub>2</sub>CO<sub>3</sub> (0.310 g, 2.250 mmol) and 1,6-dibromohexane (0.220 g, 0.900 mmol). The mixture was heated at 60 °C for 24 h. Concentration of the solvent and purification by flash-column chromatography on silica gel (hexane/EtOAc = 4:1) gave 0.151 g (68%) of the product as colourless oil. <sup>1</sup>H NMR (CDCl<sub>3</sub>, 600 MHz)  $\delta = 8.03$  (br s, 1H, NH), 7.29–7.25 (m, 1H, arom.), 7.18–7.16 (m, 1H, arom.), 7.10 (d,  $J_{h,h} = 2.4$  Hz, 1H, arom.), 6.85 (ddd,  $J_{h,h} = 8.8, 2.4, 0.4$  Hz, 1H, arom.), 6.48–6.45 (m, 1H, arom.), 4.00 (t,  $J_{h,h} = 6.4$  Hz, 2H, OCH<sub>2</sub>), 3.42 (t,  $J_{h,h} = 6.8$  Hz, 2H, CH<sub>2</sub>Br), 1.93–1.79 (m, 4H, 2 CH<sub>2</sub>), 1.55–1.49 (m, 4H, 2 CH<sub>2</sub>) ppm. <sup>13</sup>C NMR (CDCl<sub>3</sub>, 150.9 MHz)  $\delta = 153.59$  (1 arom. C), 131.00 (1 arom. C), 128.32 (1 arom. C), 124.79 (1 arom. CH), 112.93 (1 arom. CH), 111.61 (1 arom. CH), 103.54 (1 arom. CH), 102.39 (1 arom. CH), 68.57 (OCH<sub>2</sub>), 33.86 (CH<sub>2</sub>Br), 32.75 (CH<sub>2</sub>), 29.31 (CH<sub>2</sub>), 27.99 (CH<sub>2</sub>), 25.40 (CH<sub>2</sub>) ppm. C<sub>14</sub>H<sub>18</sub>BrNO (296.20): calcd. C 56.77, H 6.13, N 4.73, found C 56.48, H 6.39, N 5.02.

**4.2.2.3. 6-Bromo-N-(1H-indol-5-yl)hexanamide 3c.** To a solution of 6-bromohexanoic acid (0.174 g, 0.832 mmol) in 7 ml CH<sub>2</sub>Cl<sub>2</sub> was added 1-ethyl-3-(3-dimethylaminopropyl)carbodiimide (0.160 g, 0.832 mmol), 1-Hydroxybenzotriazole (0.112 g, 0.832 mmol) and 1H-indol-5-amine (0.100 g, 0.757 mmol). The mixture was stirred at rt for 24 h. The reaction was quenched with water, and the product was extracted with CH<sub>2</sub>Cl<sub>2</sub>. The combined organic extracts were dried over Na<sub>2</sub>SO<sub>4</sub> and the solvent was evaporated under reduced pressure. Purification by flash-column chromatography on silica gel (CH<sub>2</sub>Cl<sub>2</sub>/EtOAc = 10:1) gave 0.205 g (84%) of the product as colourless oil. <sup>1</sup>H NMR (CDCl<sub>3</sub>/CD<sub>3</sub>OD, 600 MHz)  $\delta = 7.78$ –7.77 (m, 1H, arom.), 7.33–7.30 (m, 1H, arom.), 7.23–7.19 (m, 2H, arom.), 6.46 (dd,  $J_{h,h} = 3.2, 0.8$  Hz, 1H, arom.), 3.42 (t,  $J_{h,h} = 6.7$  Hz, 2H, CH<sub>2</sub>Br), 2.37 (t,  $J_{h,h} = 7.2$  Hz, 2H, COCH<sub>2</sub>), 1.96–1.84 (m, 2H, CH<sub>2</sub>), 1.82–1.70 (m, 2H, CH<sub>2</sub>), 1.60–1.49 (m, 2H, CH<sub>2</sub>) ppm. <sup>13</sup>C NMR (CDCl<sub>3</sub>/CD<sub>3</sub>OD, 150.9 MHz)  $\delta = 172.08$  (CO), 133.51 (1 arom. C), 130.14 (1 arom. C), 128.00 (1 arom. C), 125.39 (1 arom. CH), 116.42 (1 arom. CH), 112.88 (1 arom. CH), 111.25 (1 arom. CH), 102.16 (1 arom. CH), 37.10 (COCH<sub>2</sub>), 33.77 (CH<sub>2</sub>Br), 32.56 (CH<sub>2</sub>), 27.85 (CH<sub>2</sub>), 25.00 (CH<sub>2</sub>) ppm. C<sub>14</sub>H<sub>17</sub>BrN<sub>2</sub>O (309.20): calcd. C 54.38, H 5.54, N 9.06, found C 54.01, H 5.87, N 9.13.

**4.2.2.4. (S)-Methyl 2-(6-bromohexanamido)-3-(1H-indol-2-yl)propanoate 3d.** To a solution of 6-bromohexanoic acid (0.115 g, 0.550 mmol) in 10 ml CH<sub>2</sub>Cl<sub>2</sub> was added 1-ethyl-3-(3-dimethylaminopropyl)carbodiimide (0.105 g, 0.550 mmol), 1-Hydroxybenzotriazole (0.074 g, 0.550 mmol), L-tryptophan methyl ester hydrochloride (0.127 g, 0.550 mmol) and N,N-diisopropylethylamine (0.1 ml, 0.550 mmol). The mixture was stirred at rt for 24 h. The reaction was quenched with water and the product was extracted with CH<sub>2</sub>Cl<sub>2</sub>. The combined organic extracts were dried over Na<sub>2</sub>SO<sub>4</sub> and the solvent was evaporated under reduced pressure. Purification by flash-column chromatography on silica gel (CH<sub>2</sub>Cl<sub>2</sub>/EtOAc = 10:1) gave 0.195 g (99%) of the product as colourless oil.  $[\alpha]_D^{20} = +42.7$  (c 0.400, CHCl<sub>3</sub>). <sup>1</sup>H NMR (CDCl<sub>3</sub>, 250 MHz)  $\delta = 8.17$  (br s, 1H, NH-indole), 7.53 (d,  $J_{h,h} = 7.7$  Hz, 1H, arom.), 7.36 (d,  $J_{h,h} = 7.7$  Hz, 1H, arom.), 7.23–7.09 (m, 2H, arom.), 6.98 (d,  $J_{h,h} = 2.3$  Hz, 1H, arom.), 5.94 (d,  $J_{h,h} = 7.7$  Hz, 1H, HNCO), 5.00–4.93 (m, 1H, COCH<sub>2</sub>), 3.71 (s, 3H, OCH<sub>3</sub>), 3.38–3.30 (m, 4H, CH<sub>2</sub>Br, CHCH<sub>2</sub>-indole), 2.15 (t,  $J_{h,h} = 7.1$  Hz, 2H, COCH<sub>2</sub>), 1.87–1.76 (m, 2H, CH<sub>2</sub>), 1.65–1.53 (m, 2H, CH<sub>2</sub>), 1.45–1.33 (m, 2H, CH<sub>2</sub>) ppm. <sup>13</sup>C NMR (CDCl<sub>3</sub>, 62.92 MHz)  $\delta = 172.59$  (CO), 172.28 (CO), 136.11

(1 arom. C), 127.75 (1 arom. C), 122.65 (1 arom. CH), 122.33 (1 arom. CH), 119.75 (1 arom. CH), 118.57 (1 arom. CH), 111.30 (1 arom. CH), 110.17 (1 arom. C), 52.89 (COCH<sub>2</sub>), 52.38 (OCH<sub>3</sub>), 36.24 (COCH<sub>2</sub>), 33.59 (CH<sub>2</sub>Br), 32.42 (CH<sub>2</sub>), 27.68 (CH<sub>2</sub>-indole), 27.64 (CH<sub>2</sub>), 24.15 (CH<sub>2</sub>) ppm. C<sub>18</sub>H<sub>23</sub>BrN<sub>2</sub>O<sub>3</sub> (395.29): calcd. C 54.69, H 5.86, N 7.09, found C 54.36, H 6.21, N 7.23.

#### 4.2.3. General procedure for preparation of compounds 1a–d

To a solution of norgalanthamine **2** (1 equiv) in anhydrous acetonitrile (2 mL), was added **3** (1.1 equiv) and anhydrous K<sub>2</sub>CO<sub>3</sub> (3 equiv) under argon atmosphere. After stirring at 60 °C for 24 h, the solvent was removed in vacuo. The residue was directly subjected to purification by flash column chromatography on silica gel (CH<sub>2</sub>Cl<sub>2</sub>/MeOH/NH<sub>4</sub>OH = 20/1/0.02) to give product **1**. The <sup>1</sup>H and <sup>13</sup>C NMR spectra of compounds **1a–d** are given in Supplementary data.

##### 4.2.3.1. (4a*S*,6*R*,8*aS*)-11-(6-(4-((1*H*-Indol-5-ylamino)methyl)phenoxy)hexyl)-3-methoxy-5,6,9,10,11,12-hexahydro-4*aH*-benzo[2,3]-benzofuro[4,3-*cd*]azepin-6-ol **1a**.

Yield: 73%; white crystals; mp 73–76 °C. [ $\alpha$ ]<sub>D</sub><sup>20</sup> = –45.9 (c 0.290, CHCl<sub>3</sub>). <sup>1</sup>H NMR (CDCl<sub>3</sub>, 600 MHz)  $\delta$  = 7.99 (br s, 2H, NH), 7.32–7.31 (m, 2H, arom.), 7.21–7.20 (m, 1H, arom.), 7.12–7.11 (m, 1H, arom.), 6.97–6.85 (m, 3H, arom.), 6.65–6.64 (m, 1H, arom.), 6.65 (d, *J*<sub>h,h</sub> = 8.2 Hz, 1H, H-2), 6.62 (d, *J*<sub>h,h</sub> = 8.2 Hz, 1H, H-1), 6.39–6.38 (m, 1H, arom.), 6.09 (d, *J*<sub>h,h</sub> = 10.2 Hz, 1H, H-8), 6.00 (dd, *J*<sub>h,h</sub> = 10.1, 5.0 Hz, 1H, H-7), 4.62 (br s, 1H, H-6), 4.28 (s, 2H, PhCH<sub>2</sub>), 4.15–4.12 (m, 1H, H-4*a*), 4.13 (d, *J*<sub>h,h</sub> = 15.1 Hz, 1H, H-12), 3.93 (t, *J*<sub>h,h</sub> = 6.5 Hz, 2H, OCH<sub>2</sub>), 3.83 (s, 3H, OCH<sub>3</sub>), 3.83–3.80 (m, 1H, H-12), 3.38–3.33 (m, 1H, H-10), 3.19–3.16 (m, 1H, H-10), 2.70–2.67 (m, 1H, H-5), 2.54–2.44 (m, 2H, NCH<sub>2</sub>), 2.41 (br s, 1H, OH), 2.07–1.98 (m, 2H, H-9, H-5), 1.79–1.73 (m, 2H, CH<sub>2</sub>), 1.53–1.43 (m, 5H, H-9, 2 CH<sub>2</sub>), 1.38–1.32 (m, 2H, CH<sub>2</sub>) ppm. <sup>13</sup>C NMR (CDCl<sub>3</sub>, 150.9 MHz)  $\delta$  = 158.20 (2 arom. C), 145.72 (C-3*a*), 144.03 (C-3), 142.44 (1 arom. C), 133.12 (C-12*b*), 131.87 (C-12*a*), 130.04 (1 arom. C), 128.90 (2 arom. CH), 128.72 (1 arom. C), 127.53 (C-8), 126.92 (C-7), 124.38 (1 arom. CH), 122.01 (C-1), 114.47 (2 arom. CH), 112.11 (1 arom. CH), 111.57 (1 arom. CH), 111.03 (C-2), 102.21 (1 arom. CH), 101.79 (1 arom. CH), 88.72 (C-6), 67.84 (OCH<sub>2</sub>), 62.08 (C-4*a*), 57.74 (C-12), 55.84 (OCH<sub>3</sub>), 51.49 (C-10), 51.35 (NCH<sub>2</sub>), 49.15 (PhCH<sub>2</sub>), 48.40 (C-8*a*), 32.84 (C-9), 29.90 (C-5), 29.21 (CH<sub>2</sub>), 27.34 (CH<sub>2</sub>), 27.12 (CH<sub>2</sub>), 26.01 (CH<sub>2</sub>) ppm. C<sub>37</sub>H<sub>43</sub>N<sub>3</sub>O<sub>4</sub> (593.76): calcd. C 74.84, H 7.30, N 7.09, found C 74.93, H 7.47, N 7.13.

##### 4.2.3.2. (4a*S*,6*R*,8*aS*)-11-(6-(1*H*-Indol-5-yloxy)hexyl)-3-methoxy-5,6,9,10,11,12-hexahydro-4*aH*-benzo[2,3]-benzofuro[4,3-*cd*]azepin-6-ol **1b**.

Yield: 63%; white crystals; mp 64–67 °C. [ $\alpha$ ]<sub>D</sub><sup>20</sup> = –74.6 (c 0.260, CHCl<sub>3</sub>). <sup>1</sup>H NMR (CDCl<sub>3</sub>, 600 MHz)  $\delta$  = 8.15 (br s, 1H, NH), 7.26 (s, 1H, arom.), 7.17 (t, *J*<sub>h,h</sub> = 5.5 Hz, 1H, arom.), 7.09 (d, *J*<sub>h,h</sub> = 2.4 Hz, 1H, arom.), 6.84 (dd, *J*<sub>h,h</sub> = 8.8, 2.4 Hz, 1H, arom.), 6.65 (d, *J*<sub>h,h</sub> = 8.2 Hz, 1H, H-2), 6.62 (d, *J*<sub>h,h</sub> = 8.2 Hz, 1H, H-1), 6.47–6.46 (m, 1H, arom.), 6.08 (d, *J*<sub>h,h</sub> = 10.2 Hz, 1H, H-8), 6.00 (dd, *J*<sub>h,h</sub> = 10.2, 5.1 Hz, 1H, H-7), 4.61 (br s, 1H, H-6), 4.16–4.13 (m, 1H, H-4*a*), 4.14 (d, *J*<sub>h,h</sub> = 15.2 Hz, 1H, H-12), 3.98 (t, *J*<sub>h,h</sub> = 6.5 Hz, 1H, OCH<sub>2</sub>), 3.83 (d, *J*<sub>h,h</sub> = 15.2 Hz, 1H, H-12), 3.82 (s, 3H, OCH<sub>3</sub>), 3.39–3.34 (m, 1H, H-10), 3.20–3.18 (m, 1H, H-10), 2.70–2.66 (m, 1H, H-5), 2.55–2.45 (m, 2H, NCH<sub>2</sub>), 2.41 (br s, 1H, OH), 2.07–1.98 (m, 2H, H-9, H-5), 1.81–1.77 (m, 2H, CH<sub>2</sub>), 1.53–1.46 (m, 5H, H-9, 2 CH<sub>2</sub>), 1.40–1.31 (m, 2H, CH<sub>2</sub>) ppm. <sup>13</sup>C NMR (CDCl<sub>3</sub>, 150.9 MHz)  $\delta$  = 153.53 (2 arom. C), 145.72 (C-3*a*), 144.07 (C-3), 133.09 (C-12*b*), 130.90 (C-12*a*), 128.24 (1 arom. C), 127.56 (C-8), 126.87 (C-7), 124.79 (1 arom. CH), 122.09 (C-1), 112.84 (1 arom. CH), 111.59 (1 arom. CH), 111.06 (C-2), 103.36 (1 arom. CH), 102.27 (1 arom. CH), 88.70 (C-6), 68.59 (OCH<sub>2</sub>), 62.06 (C-4*a*), 57.68 (C-12), 55.83 (OCH<sub>3</sub>), 51.46 (C-10), 51.33 (NCH<sub>2</sub>), 48.36 (C-8*a*), 32.76 (C-9), 29.89 (C-5), 29.38 (CH<sub>2</sub>), 27.27 (CH<sub>2</sub>), 27.14 (CH<sub>2</sub>), 26.06 (CH<sub>2</sub>)

ppm. C<sub>30</sub>H<sub>36</sub>N<sub>2</sub>O<sub>4</sub> (488.62): calcd. C 73.74, H 7.43, N 5.73, found C 74.02, H 7.72, N 5.68.

##### 4.2.3.3. *N*-(1*H*-Indol-5-yl)-6-((4a*S*,6*R*,8*aS*)-6-hydroxy-3-methoxy-5,6,9,10-tetrahydro-4*aH*-benzo[2,3]-benzofuro[4,3-*cd*]azepin-11(12*H*)-yl)hexanamide **1c**.

Yield: 47%; white crystals; mp 101–104 °C. [ $\alpha$ ]<sub>D</sub><sup>20</sup> = –47.6 (c 0.250, CHCl<sub>3</sub>). <sup>1</sup>H NMR (CDCl<sub>3</sub>/CD<sub>3</sub>OD, 600 MHz)  $\delta$  = 7.80 (d, *J*<sub>h,h</sub> = 1.8 Hz, 1H, arom.), 7.33 (d, *J*<sub>h,h</sub> = 8.6 Hz, 1H, arom.), 7.23–7.21 (m, 2H, arom.), 6.66 (d, *J*<sub>h,h</sub> = 8.2 Hz, 1H, H-2), 6.63 (d, *J*<sub>h,h</sub> = 8.2 Hz, 1H, H-1), 6.45 (d, *J*<sub>h,h</sub> = 2.6 Hz, 1H, arom.), 6.07 (d, *J*<sub>h,h</sub> = 10.2 Hz, 1H, H-8), 5.99 (dd, *J*<sub>h,h</sub> = 10.2, 5.1 Hz, 1H, H-7), 4.60 (br s, 1H, H-6), 4.16–4.14 (m, 1H, H-4*a*), 4.15 (d, *J*<sub>h,h</sub> = 15.4 Hz, 1H, H-12), 3.85 (d, *J*<sub>h,h</sub> = 15.4 Hz, 1H, H-12), 3.83 (s, 3H, OCH<sub>3</sub>), 3.38–3.33 (m, 1H, H-10), 3.20–3.19 (m, 1H, H-10), 2.65–2.62 (m, 1H, H-5), 2.57–2.47 (m, 2H, NCH<sub>2</sub>), 2.36 (t, *J*<sub>h,h</sub> = 7.4 Hz, 2H, CH<sub>2</sub>CO), 2.08–2.00 (m, 2H, H-5, H-9), 1.76–1.71 (m, 2H, CH<sub>2</sub>), 1.57–1.55 (m, 3H, H-9, CH<sub>2</sub>), 1.40–1.34 (m, 2H, CH<sub>2</sub>) ppm. <sup>13</sup>C NMR (CDCl<sub>3</sub>/CD<sub>3</sub>OD, 150.9 MHz)  $\delta$  = 172.66 (CO), 145.93 (C-3*a*), 144.40 (C-3), 133.61 (1 arom. C), 133.59 (C-12*b*), 130.10 (C-12*a*), 130.32 (1 arom. C), 128.01 (1 arom. C), 127.62 127.56 (C-8), 126.99 (C-7), 125.52 (1 arom. CH), 122.65 (C-1), 116.29 (1 arom. CH), 112.74 (1 arom. CH), 111.51 (C-2), 111.30 (1 arom. CH), 101.98 (1 arom. CH), 88.57 (C-6), 61.97 (C-4*a*), 57.61 (C-12), 55.98 (OCH<sub>3</sub>), 51.51 (C-10), 51.44 (NCH<sub>2</sub>), 48.34 (C-8*a*), 36.89 (CH<sub>2</sub>CO), 32.56 (C-9), 29.99 (C-5), 26.81 (CH<sub>2</sub>), 25.45 (CH<sub>2</sub>), 25.65 (CH<sub>2</sub>) ppm. C<sub>30</sub>H<sub>35</sub>N<sub>3</sub>O<sub>4</sub> (501.62): calcd. C 71.83, H 7.03, N 8.38, found C 71.97, H 6.78, N 8.49.

##### 4.2.3.4. (*S*)-Methyl-3-(1*H*-indol-3-yl)-2-(6-((4a*S*,6*R*,8*aS*)-6-hydroxy-3-methoxy-5,6,9,10-tetrahydro-4*aH*-benzo[2,3]-benzofuro[4,3-*cd*]azepin-11(12*H*)-yl)hexanamido)propanoate **1d**.

Yield: 76%; white crystals; mp 86–89 °C. [ $\alpha$ ]<sub>D</sub><sup>20</sup> = –18.6 (c 0.290, CHCl<sub>3</sub>). <sup>1</sup>H NMR (CDCl<sub>3</sub>, 600 MHz)  $\delta$  = 8.32 (br s, 1H, NH-indole), 7.51 (d, *J*<sub>h,h</sub> = 8.0 Hz, 1H, arom.), 7.35 (d, *J*<sub>h,h</sub> = 8.2 Hz, 1H, arom.), 7.19 (dt, *J*<sub>h,h</sub> = 7.0, 1.1 Hz, 1H, arom.), 7.11 (dt, *J*<sub>h,h</sub> = 7.1, 1.0 Hz, 1H, arom.), 6.96 (d, *J*<sub>h,h</sub> = 2.3 Hz, 1H, arom.), 6.65 (d, *J*<sub>h,h</sub> = 8.2 Hz, 1H, H-2), 6.61 (d, *J*<sub>h,h</sub> = 8.2 Hz, 1H, H-1), 6.07 (d, *J*<sub>h,h</sub> = 10.2 Hz, 1H, H-8), 6.01 (dd, *J*<sub>h,h</sub> = 10.2, 5.0 Hz, 1H, H-7), 5.97 (d, *J*<sub>h,h</sub> = 7.9 Hz, 1H, NH), 4.95 (dq, *J*<sub>h,h</sub> = 7.9, 5.4 Hz, 1H, CHCH<sub>2</sub>), 4.61 (br s, 1H, H-6), 4.14 (br s, 1H, H-4*a*), 4.13 (d, *J*<sub>h,h</sub> = 15.4 Hz, 1H, H-12), 3.83 (s, 3H, OCH<sub>3</sub>), 3.81 (d, *J*<sub>h,h</sub> = 15.4 Hz, 1H, H-12), 3.70 (s, 3H, COOCH<sub>3</sub>), 3.37–3.27 (m, 3H, H-10, CHCH<sub>2</sub>), 3.16 (d, *J*<sub>h,h</sub> = 14.0 Hz, 1H, H-10), 2.70–2.67 (m, 1H, H-5), 2.51–2.40 (m, 2H, NCH<sub>2</sub>), 2.14–2.11 (m, 2H, CH<sub>2</sub>CONH), 2.05–1.98 (m, 2H, H-9, H-5), 1.60–1.55 (m, 2H, CH<sub>2</sub>), 1.51 (d, *J*<sub>h,h</sub> = 13.6 Hz, 1H, H-9), 1.48–1.43 (m, 2H, CH<sub>2</sub>), 1.27–1.22 (m, 2H, CH<sub>2</sub>) ppm. <sup>13</sup>C NMR (CDCl<sub>3</sub>, 150.9 MHz)  $\delta$  = 172.52 (2 CO), 145.78 (C-3*a*), 144.16 (C-3), 136.09 (C-12*b*), 133.11 (C-12*a*), 127.69 (C-8), 127.67 (C-7), 126.82 (1 arom. C), 126.78 (1 arom. C), 122.74 (1 arom. CH), 122.21 (C-1), 122.15 (1 arom. CH), 122.04 (1 arom. C), 119.63 (1 arom. CH), 118.55 (1 arom. CH), 111.30 (1 arom. CH), 110.05 (1 arom. C), 88.72 (C-6), 62.06 (C-4*a*), 57.60 (C-12), 55.88 (OCH<sub>3</sub>), 52.76 (CHCH<sub>2</sub>), 52.38 (COOCH<sub>3</sub>), 51.45 (C-10), 51.08 (NCH<sub>2</sub>), 48.35 (C-8*a*), 36.40 (CH<sub>2</sub>CO), 32.73 (C-9), 29.91 (C-5), 27.62 (CHCH<sub>2</sub>), 26.94 (CH<sub>2</sub>), 26.82 (CH<sub>2</sub>), 25.26 (CH<sub>2</sub>) ppm. C<sub>34</sub>H<sub>41</sub>N<sub>3</sub>O<sub>5</sub> (587.71): calcd. C 69.48, H 7.03, N 7.15, found C 69.32, H 7.24, N 7.21.

#### 4.3. Assessment of AChE inhibitory activity

AChE activity was assayed as described by Ellman et al.<sup>60</sup> with some modifications.<sup>61</sup> Fifty  $\mu$ L of *T. californica* AChE (Sigma–Aldrich) in buffer phosphate (pH 7.6) and 50  $\mu$ L of the tested compounds (4–500  $\mu$ M in methanol) dissolved in 700  $\mu$ L in the same buffer. The mixtures were incubated for 30 min at room temperature before the addition of 100  $\mu$ L of the substrate solution (0.5 M DTNB, 0.6 mM ATCI in buffer, pH 7.6). The absorbance was read in

Shimadzu spectrophotometer at 405 nm after three minutes. Enzyme activity was calculated as a percentage compared to an assay using a buffer without any inhibitor using nonlinear regression. IC<sub>50</sub> values are means ± SD of three individual determinations each performed in triplicate.

#### 4.4. Visualization of ligand–AChE interactions

The interactions between the ligands and AChE were visualized by YASARA v.12.11.25.<sup>62</sup> Four types of interactions were considered: hydrogen bonds, hydrophobic interactions,  $\pi$ – $\pi$  stacking and cation– $\pi$  interactions. For visualizing of hydrogen bonds, an extended selection was used to include all hydrogen bonding partners of the bound ligand. The  $\pi$ – $\pi$  stacking, the hydrophobic and cation– $\pi$  interactions are shown at distances below 5.0 Å.

#### Acknowledgement

This work was supported by the Medical Science Council (Grant 2-S/2013).

#### Supplementary data

Supplementary data (the structures and IC<sub>50</sub> values of the GAL derivatives used in the docking study. The <sup>1</sup>H and <sup>13</sup>C NMR spectra of compounds **1a–d**) associated with this article can be found, in the online version, at <http://dx.doi.org/10.1016/j.bmc.2015.07.058>.

#### References and notes

- Alzheimer's Association *Alzheimers Dement.* **2014**, *10*, e47.
- Franco, R.; Cedazo-Minguez, A. *Front. Pharmacol.* **2014**, *5*, 146.
- Lannfeld, L.; Moller, C.; Basun, H.; Osswald, G.; Sehlín, D.; Satlin, A.; Logovinsky, V.; Gellerfors, P. *Alzheimers Res. Ther.* **2014**, *6*, 16.
- Lannfeld, L.; Relkin, N. R.; Siemers, E. R. *J. Intern. Med.* **2014**, *275*, 284.
- Anand, P.; Singh, B. *Arch. Pharm. Res.* **2013**, *36*, 375.
- Lu, S. H.; Wu, J. W.; Liu, H. L.; Zhao, J. H.; Liu, K. T.; Chuang, C. K.; Lin, H. Y.; Tsai, W. B.; Ho, Y. J. *Biomed. Sci.* **2011**, *18*, 8.
- Lasner, C. J.; Lee, J. M. *J. Neurophathol. Exp. Neurol.* **1998**, *57*, 719.
- Inestrosa, N. C.; Alvarez, A.; Perez, C. A.; Moreno, R. D.; Vicente, M.; Linker, C.; Casanueva, O. I.; Soto, C.; Garrido, J. *Neuron* **1996**, *16*, 881.
- Mattson, M. P. *Nature* **2004**, *430*, 631.
- Dinamarca, M. C.; Sagal, J. P.; Quintanilla, R. A.; Godoy, J. A.; Arrazola, M. S.; Inestrosa, N. C. *Mol. Neurodegener.* **2010**, *5*, 4.
- Harel, M.; Schalk, I.; Ehret-Sabatier, L.; Bouet, F.; Goeldner, M.; Hirth, C.; Axelsen, P. H.; Silman, I.; Sussman, J. L. *Proc. Natl. Acad. Sci. U.S.A.* **1993**, *90*, 9031.
- Ordentlich, A.; Barak, D.; Kronman, C.; Flashner, Y.; Leitner, M.; Segall, Y.; Ariel, N.; Cohen, S.; Velan, B.; Shafferman, A. *J. Biol. Chem.* **1993**, *268*, 17083.
- Ordentlich, A.; Barak, D.; Kronman, C.; Ariel, N.; Segall, Y.; Velan, B.; Shafferman, A. *J. Biol. Chem.* **1998**, *273*, 19509.
- Radic, Z.; Pickering, N. A.; Vellom, D. C.; Camp, S.; Taylor, P. *Biochemistry* **1993**, *32*, 12074.
- Sussman, J. L.; Harel, M.; Frolow, F.; Oefner, C.; Goldman, A.; Tokar, L.; Silman, I. *Science* **1991**, *253*, 872.
- Kitz, R. J.; Braswell, L. M.; Ginsburg, S. *Mol. Pharmacol.* **1970**, *6*, 108.
- De Ferrari, G. V.; Canales, M. A.; Shin, I.; Weiner, L. M.; Silman, I.; Inestrosa, N. C. *Biochemistry* **2001**, *40*, 10447.
- Johnson, G.; Moore, S. W. *Biochem. Biophys. Res. Commun.* **2004**, *319*, 448.
- Johnson, G.; Moore, S. W. *Curr. Pharm. Des.* **2006**, *12*, 217.
- Viayna, E.; Sabate, R.; Munoz-Torrero, D. *Curr. Top. Med. Chem.* **2006**, *13*, 2006.
- Camps, P.; Formosa, X.; Galdeano, C.; Munoz-Torrero, D.; Ramirez, L.; Gomez, E.; Isambert, N.; Lavilla, R.; Badia, A.; Clos, M. V.; Bartolini, M.; Mancini, F.; Andrisano, V.; Arce, M. P.; Rodrigues-Franco, M. I.; Huertas, O.; Dafni, T.; Luque, F. J. *J. Med. Chem.* **2009**, *52*, 5365.
- Yu, L.; Cao, R.; Yi, W.; Yan, Q.; Chen, Z.; Ma, L.; Peng, W.; Song, H. *Bioorg. Med. Chem. Lett.* **2010**, *20*, 3254.
- Leon, R.; Marco-Contelles, J. *Curr. Med. Chem.* **2011**, *18*, 552.
- Simoni, E.; Daniele, S.; Bottegoni, G.; Pizzirani, D.; Trincavelli, M. L.; Goldoni, L.; Tarozzo, G.; Reggiani, A.; Martini, C.; Piomelli, D.; Melchiorre, C.; Rosini, M.; Cavalli, A. *J. Med. Chem.* **2012**, *55*, 9708.
- Nepovimova, E.; Uliassi, E.; Korabechy, J.; Pena-Altamira, L. E.; Samez, S.; Pesaresi, A.; Garcia, G. E.; Bartolini, M.; Andrisano, V.; Bergamini, C.; Fato, R.; Lamba, D.; Roberti, M.; Kuca, K.; Monti, B.; Bolognesi, M. L. *J. Med. Chem.* **2014**, *57*, 8576.
- Bartolucci, C.; Perola, E.; Pilger, C.; Fels, G.; Lamba, D. *Proteins* **2001**, *42*, 182.
- Cheung, J.; Rudolph, M. J.; Burshteyn, F.; Cassidy, M. S.; Gary, E. N.; Love, J.; Franklin, M. C.; Height, J. J. *J. Med. Chem.* **2012**, *55*, 10282.
- Heinrich, M.; Teoh, H. L. *J. Ethnopharm.* **2004**, *92*, 147.
- Paskov, D. S. *Nivalin: Pharmacology and Clinical Application*; Medicina i Fizkultura: Sofia, Bulgaria, 1959.
- Paskov, D. S. *Series Exp. Biol. Med., Sofia* **1957**, *1*, 29.
- Bubeva-Ivanova, L. *Pharmacia (Sofia)* **1957**, *2*, 23.
- Nastev, G. *Cult. Med. (Roma)* **1960**, *15*, 87.
- Der Stoyanov, E. A. *Anaesthetist* **1964**, *13*, 217.
- Paskov, D. S. In *Handbook of Experimental Pharmacology*; Kharkevich, D. A., Ed.; Springer: Berlin-Heidelberg, New York, Tokyo, 1986; pp 653–672.
- Parys, W. *Alzheimer's Rep.* **1998**, *53*, S19.
- Farlow, M. R. *Clin. Ther.* **2001**, *23*, A13.
- Marco-Contelles, J.; Rodríguez, C.; Carreiras, M. C.; Villarroya, M.; García, A. G. *Chem. Rev.* **2006**, *106*, 116.
- Pereira, E. F.; Reinhardt-Maelicke, S.; Schratzenholz, A.; Maelicke, A.; Albuquerque, E. X. *J. Pharmacol. Exp. Ther.* **1993**, *265*, 1474.
- Storch, A.; Schratzenholz, A.; Cooper, J. C.; Abdel Ghani, E. M.; Gutbrod, O.; Weber, K. H.; Reinhardt, S.; Lobron, C.; Hermesen, B.; Soskic, V.; Pereira, E. F. R.; Albuquerque, E. X.; Methfessel, C.; Maelicke, A. *Eur. J. Pharm.* **1995**, *290*, 207.
- Schrattenholz, A.; Pereira, E. F.; Roth, U.; Weber, K. H.; Albuquerque, E. X.; Maelicke, A. *Mol. Pharmacol.* **1996**, *49*, 1.
- Albuquerque, E. X.; Alkondon, M.; Pereira, E. F.; Castro, C. F.; Schratzenholz, A.; Barbosa, C. T.; Bonfante-Canarcas, R.; Aracava, Y.; Eisenberg, H. M.; Maelicke, A. *J. Pharmacol. Exp. Ther.* **1997**, *280*, 1117.
- Dajas-Bailador, F. A.; Heimala, K.; Wonnacott, S. *Mol. Pharmacol.* **2003**, *64*, 1217.
- Takata, K.; Kitamura, Y.; Saeki, M.; Terada, M.; Kagitani, S.; Kitamura, R.; Fujikawa, Y.; Maelicke, A.; Tomimoto, H.; Taniguchi, T.; Shimohama, S. *J. Biol. Chem.* **2010**, *285*, 40180.
- Han, S. Y.; Sweeney, J. E.; Bachman, E. S.; Schweiger, E. J.; Forloni, G.; Coyle, J. T.; Davis, B. M.; Joullié, M. M. *Eur. J. Med. Chem.* **1992**, *27*, 673.
- Bores, G. M.; Kosley, R. W. *Drugs Future* **1996**, *21*, 621.
- Mary, A.; Renko, D. Z.; Guillou, C.; Thal, C. *Bioorg. Med. Chem.* **1835**, 1998, 6.
- Guillou, C.; Mary, A.; Renko, D. Z.; Thal, C. *Bioorg. Med. Chem. Lett.* **2000**, *10*, 637.
- Treu, M.; Jordis, U.; Mereiter, K. *Heterocycles* **2001**, *55*, 1727.
- Poschalko, A.; Welzig, S.; Treu, M.; Nerdinger, S.; Mereiter, K.; Jordis, U. *Tetrahedron* **2002**, *58*, 1513.
- Herlem, D.; Martin, M. T.; Thal, C.; Guillou, C. *Bioorg. Med. Chem. Lett.* **2003**, *13*, 2389.
- Guillou, C.; Mary, A.; Renko, D. Z.; Gras, E.; Thal, C. *Bioorg. Med. Chem. Lett.* **2000**, *10*, 637.
- Greenblatt, H. M.; Guillou, C.; Guenard, D.; Argaman, A.; Botti, S.; Badet, B.; Thal, C.; Silman, I.; Sussman, J. L. *J. Am. Chem. Soc.* **2004**, *126*, 15405.
- Bartolucci, C.; Haller, L. A.; Jordis, U.; Fels, G.; Lamba, D. *J. Med. Chem.* **2010**, *53*, 745.
- Kozurkova, M.; Hamulakova, S.; Gazova, Z.; Paulikova, H.; Kristian, P. *Pharmaceuticals* **2011**, *4*, 382.
- Bolea, I.; Juárez-Jiménez, J.; de los Ríos, C.; Chioua, M.; Pouplana, R.; Luque, F. J.; Unzeta, M.; Marco-Contelles, J.; Samadi, A. *J. Med. Chem.* **2011**, *54*, 8251.
- Czollner, L.; Kälz, B.; Welzig, S.; Frantsits, W. J.; Jordis, U.; Fröhlich, J. Patent WO 2005/030333 A2, 2005.
- Jia, P.; Sheng, R.; Zhang, J.; Fang, L.; He, Q.; Yang, B.; Hu, Y. *Eur. J. Med. Chem.* **2009**, *44*, 772.
- Jones, G.; Willett, P.; Glen, R. C.; Leach, A. R.; Taylor, R. *J. Mol. Biol.* **1997**, *267*, 727.
- Mary, A.; Renko, D. Z.; Guillou, C.; Thal, C. *Tetrahedron Lett.* **1997**, *38*, 5151.
- Ellman, G. L.; Courtney, K. D.; Andreas, V., Jr.; Featherstone, R. M. *Biochem. Pharmacol.* **1961**, *7*, 88.
- Ortiz, J.; Berkov, S.; Pigni, N.; Theoduloz, C.; Roitman, G.; Tapia, A.; Bastida, J.; Feresin, G. E. *Molecules* **2012**, *17*, 13473.
- Krieger, E.; Koramann, G.; Vriend, G. *Proteins* **2002**, *47*, 393.
- Lyskov, S.; Gray, J. J. *Nucleic Acids Res.* **2008**, *36*, W233.
- Kellenberger, E.; Rodrigo, J.; Muller, P.; Rognan, D. *Proteins* **2004**, *57*, 225.
- Perola, E.; Walters, W. P.; Charifson, P. S. *Proteins* **2004**, *56*, 235.
- Sticht, H.; Bayer, P.; Willbold, D.; Dames, S.; Hilbich, C.; Beyreuther, K.; Frank, R. W.; Rosch, P. *Eur. J. Biochem.* **1995**, *233*, 293.